COMPARISON OF FLAW GROWTH CHARACTERISTICS UNDER CRYOGENIC PROOF AND AMBIENT TEST CONDITIONS FOR APOLLO TITANIUM PRESSURE VESSELS

By
W. D. Bixler

Prepared for

NATIONAL AERONAUTICS AND SPACE ADMINISTRATION

Contract NAS 9-10265

THE BOEING COMPANY

FINAL REPORT

COMPARISON OF FLAW GROWTH CHARACTERISTICS UNDER CRYOGENIC PROOF AND AMBIENT TEST CONDITIONS FOR APOLLO TITANIUM PRESSURE VESSELS

By

W. D. Bixler

Prepared for

NATIONAL AERONAUTICS AND SPACE ADMINISTRATION

January 1970

Contract NAS9-10265

Technical Management

NASA Manned Spacecraft Center

Houston, Texas

G. M. Ecord

AEROSPACE SYSTEMS DIVISION

The Boeing Company

Seattle, Washington

COMPARISON OF FLAW GROWTH CHARACTERISTICS UNDER CRYOGENIC PROOF AND AMBIENT TEST CONDITIONS FOR APOLLO TITANIUM PRESSURE VESSELS

By

W. D. Bixler

ABSTRACT

The flaw growth characteristics of 6Al-4V titanium under cyrogenic proof and ambient test conditions were experimentally determined using surface flawed fracture specimens. Analysis of the specimens was based on linear elastic fracture mechanics. It was concluded from these results that flaw growth occurs during cryogenic proof and ambient test conditions for specific combinations of stress and flaw size.

FOREWORD

The possibility of significant flaw growth during cryogenic proof test of thin walled 6Al-4V titanium pressure vessels prompted NASA/MSC Houston, Texas, to initiate a study aimed at determining the flaw growth characteristics of Apollo tanks under cryogenic proof and ambient test conditions. NASA requested the Aerospace Systems Division of The Boeing Company to conduct this investigation. A seven week program was conducted under NASA Contract NAS9-10265 and the results are reported herein. The work was administered under the direction of Mr. G. M. Ecord at NASA/MSC.

Boeing personnel who participated in this investigation include J. N. Masters, Program Supervisor and W. D. Bixler, Technical Leader. Structural testing of the specimens was conducted by A. A. Ottlyk and the technical illustrations were prepared by D. G. Good.

The information contained in this report is released as Boeing Document D2-121700-1.

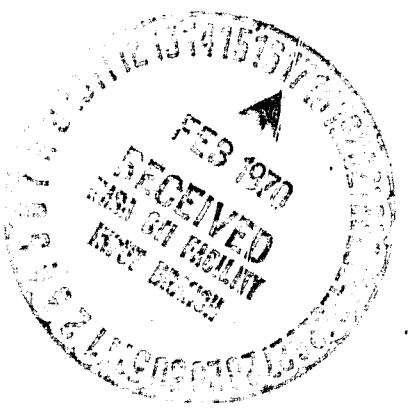

SUMMARY

The objective of this program was to determine the growth characteristics of flaws in 6Al-4V titanium when subjected to cryogenic proof and ambient test conditions. This was accomplished by testing surface flawed fracture specimens in liquid nitrogen at -320°F and in air at room temperature. Some specimens were failed in liquid nitrogen to determine the plane strain fracture toughness while others were loaded to a predetermined cryogenic proof stress level and then unloaded. The specimens that were unloaded were either observed for flaw growth, caused by the proof stress cycle, or subjected to a subsequent room temperature stress cycle and then observed for flaw growth. Additional specimens were subjected only to a room temperature stress cycle and then observed for flaw growth. The amount of flaw growth under all loading conditions tested was compared.

The results of these tests indicated that

1) significant flaw growth does occur during cryogenic proof testing at -320°F when the stress intensity exceeds about 85 percent of K_{Ic} at -320°,

2) reduced pressure vessel capability can be expected if the vessel just passes a 168 ksi cryogenic proof test at -320°F and is then subjected to a room temperature proof test to 140 ksi, and

3) no measurable flaw growth results when a pressure vessel is subjected to a room temperature stress of 105 ksi after barely passing a 168 ksi cryogenic proof test at -320°F.

TABLE OF CONTENTS

LIST OF ILLUSTRATIONS

LIST OF TABLES

1.0 INTRODUCTION

Experimental data presented in Reference 1 shows that less than critical, deep flaws in thin section titanium pressure vessels at high cyclic stresses may grow an unexpectedly large amount under ambient conditions. The relative growth for deep flaws in thin sections of the same material under cryogenic conditions is not known. It can be theorized that a deep flaw may pass a cryogenic proof test yet experience a large amount of growth during ambient cyclic service and fail unexpectedly unless the flaw growth characteristics during the cryogenic proof test are comparable to the ambient characteristics. Since acceptance tests for some Apollo pressure vessels include a cryogenic proof test rather than an ambient proof test, the flaw growth characteristics must be determined for deep flaws subjected to a cryogenic test.

This experimental investigation was divided into four parts designed to compare the flaw growth characteristics of flaws under cryogenic proof and ambient test conditions. The objective of each test part is indicated below:

Part I — Determine the plane strain fracture toughness of the tank material in liquid nitrogen at -320°F so that the critical flaw size at a stress of 168 ksi can be calculated.

Part II — Determine the maximum flaw size that can successfully pass a -320°F proof cycle to 168 ksi in liquid nitrogen.

Part III — Determine if any flaw growth occurs due to a room temperature stress cycle at about the maximum operating stress level of 98 to 105 ksi for an initial flaw size that would pass a cryogenic proof test.

Part IV — Determine if any flaw growth occurs due to a room temperature stress cycle to about 98 to 105 ksi after having successfully passed a -320°F proof test to 168 ksi.

2.0 MATERIAL

The material used to fabricate the fracture specimens for this experimental test program was from an Apollo Service Module SPS tank. This 6Al-4V STA titanium forging was surplus material that was used in the experimental investigation of Reference 2. As reported in Reference 2, this forging exhibited a room temperature plane strain fracture toughness of 46.6 ksi $\sqrt{in.}$

3.0 PROCEDURES

Precracked surface flaw specimens were used for all static toughness and flaw growth evaluation tests. Flaws were made by electric discharge machining (EDM) a starter notch, and extending the notch by low stress tension fatigue. The fatigue extension was accomplished at a maximum gross stress of either 30 or 40 ksi at 1800 cpm. The number of cycles required for precracking varied depending upon the initial notch dimensions, but was generally about 20,000 cycles. All precracking was done in air at room temperature.

Overall dimensions of the specimen were tailored to the size and shape of the available forging. The specimen configuration is shown in Figure 1. The test section thickness was machined to 0.033 inches, to simulate an actual Apollo tank wall thickness.

All fracture specimens were loaded in a 12,000 pound universal testing machine at a linear rate of 900 lb/minute (approximately 34 ksi/minute). This rate was selected to simulate the loading rate of a typical cryogenic proof test. For specimens that did not fail, the load was dropped immediately to zero upon reaching a predetermined value. Each specimen was instrumented to determine the crack opening displacement as described in Reference 2.

The approach used in testing the specimens is presented below for each test part:

Part 1

Specimens with initial flaw sizes that would cause failure between 140 to 190 ksi (to bracket a cryogenic proof stress of 168 ksi) were positioned, one at a time, in the testing machine and then submerged in liquid nitrogen. After temperature stabilization to -320^{o}F (indicated by stabilization of the flaw opening displacement strain gage), the specimen was pulled to failure.

Part II

Specimens with varying initial flaw sizes were loaded at cryogenic temperature (-320°F) to a stress level of 168 ksi, unloaded immediately, and then low stress tension fatigued in air at room temperature to mark the flaw front. The specimens were then failed and observed for flaw growth.

Part III

Specimens, with initial flaw sizes targeted at the critical flaw size at a cryogenic proof stress of 168 ksi, were loaded at room temperature to stress levels between 80 and 140 ksi (to bracket the maximum operating stress level of 98 to 105 ksi), unloaded immediately, marked and failed. These specimens were then observed for flaw growth.

Part IV

Specimens, with initial flaw sizes targeted at slightly less then the critical flaw size at a cryogenic proof stress of 168 ksi, were loaded at cryogenic temperature (-320°F) to 168 ksi, immediately unloaded, then loaded at room temperature to a stress level between 80 and 120 ksi. After reaching the predetermined room temperature stress level the specimens were immediately unloaded, marked, failed and observed for flaw growth.

During all four testing parts the flaw opening displacement was observed while load was applied to the specimen.

4.0 DATA RESULTS AND ANALYSIS

The data obtained was analyzed using the Kobayashi solution for stress intensity as shown below:

$$K_I = 1.95\sigma(a/Q)^{1/2}M_K$$

where

K_I = applied stress intensity

σ = gross stress

a = flaw depth

Q = flaw shape parameter

M_K = Kobayashi's deep flaw magnification factor

The flaw shape parameter and deep flaw magnification factor are the same ones described and presented in Reference 2. Because of the experimental differences in flaw size and flaw shape between specimens, all data points are presented as functions of stress, σ, and a flaw size/shape parameter, $(a/Q)^{1/2}M_K$. The flaw size/shape parameter can account for different flaw depths (a), depth-to-width ratios (a/2c), stress-to-yield stress ratios (σ / σ_{ys}) and deep flaw magnification factors (M_K, a function of a/t) and is therefore very convenient in presenting experimental surface flaw fracture data. All data results are tabulated in Tables I through IV.

Part I

The objective of this phase of the program was to determine the plane strain fracture toughness of the tank material in liquid nitrogen at -320°F so that the critical flaw size at a stress of 168 ksi can be calculated. Figure 2 presents the data obtained during this testing phase. A total of nine specimens failed during the testing; some were obtained from Part II and IV testing where the specimens did not successfully pass the cryogenic proof cycle because of excessive flaw sizes.

An average plane strain fracture toughness of 43.2 ksi $\sqrt{in}$, based on the initial flaw size, was obtained at -320°F in liquid nitrogen. The data scatter amounted to about ± 10 percent. A rough estimate of the flaw size at the instant of unstable crack propagation was made based on some of the flaw opening displacement data for these specimens. Flaw opening displacement is a result of plastic yielding at the crack tip and flaw growth. With flaws that are deep with respect to the thickness, the amount of plastic yielding that takes place becomes significant and consequently its affect on flaw opening displacement. At present, no suitable means have been developed to determine the amount of flaw opening displacement due to plastic yielding. In addition to the plastic yielding problem, a significant amount of data scatter was observed in the flaw opening displacement data at -320°F, confounding the issue so that only a rough estimate of the flaw growth during loading for the fracture toughness specimens could be made. As indicated in Parts II and IV of this preliminary report, definite flaw growth was observed in specimens at -320°F that were unloaded just prior to failure and then marked and failed.

A scatter band estimate of the possible flaw size present at plane strain fracture is also shown in Figure 2. The final flaw size could be anywhere within these limits, keeping in mind that the upper limit at $K_{Ic} \approx 49$ ksi $\sqrt{in}$ is only a rough estimate.

This forging has a plane strain fracture toughness of 46.6 ksi $\sqrt{in}$ as determined in Reference 2 at room temperature, based on the initial flaw size. This is only slightly higher than the cryogenic value. The critical flaw size/shape parameter, $(a/Q)^{1/2}M_K$, at 168 ksi was determined to be 0.1320 $\sqrt{in}$ at -320°F based on the initial flaw size prior to proof. This translates into a flaw depth of 0.0143 inches for a long flaw (Q = 1.0) and a nominal thickness of 0.033 inches.

Part II

The objective of this phase of the program was to determine the maximum flaw size that can successfully pass a -320°F proof cycle to 168 ksi in liquid nitrogen. Figure 3 presents the data obtained during this testing phase. A total of four specimens successfully passed the cryogenic proof test during this testing phase. Specimens tested in Part IV can be also used here to determine the maximum flaw size that can get through a cryogenic proof since they also had to pass this proof test prior to being loaded to an operating stress at room temperature. Of the four specimens tested in Part II only one showed signs of growth during loading, specimen #6. Two of the specimens tested during Part IV, specimens #14 and #8, exhibited significant growth which could have occurred during proof or during the room temperature operating cycle put on after the proof (see photos in Figure 6). The appearance of both specimens after the cryogenic proof indicated growth indeed had taken place. A significant dimple had developed on the back side of specimens (especially #14), opposite the flaw front. Past experience with specimens of similar flaw sizes and thicknesses has indicated that this amount of dimpling relates to significant flaw growth. An additional factor supporting this conclusion was the significant amount of flaw opening displacement that occurred with specimen #14. It is believed that specimen #14 would have failed if the stress had been increased by a few ksi.

From this information plus that supplied by the other specimens, the maximum initial flaw size/shape parameter that can successfully pass a -320°F cryogenic proof is slightly less than 0.1320 $\sqrt{in}$. This translates into a flaw depth of 0.0143 inches for a long flaw (Q = 1.0) and a nominal thickness of 0.033 inches. It is also apparent that a no-growth line at about 85 percent of K_{Ic} at -320°F exists, because specimens #16, #17, #18 and #19 did not indicate growth during the cryogenic proof. More data is required to determine the maximum flaw size that could be present after barely passing a 168 ksi cryogenic proof.

The only data point left unexplained is specimen #5, which did not exhibit any growth. The only explanation offered is that it probably would have demonstrated a higher toughness than the other specimens tested if loaded to failure.

Part III

The objective of this phase of the program was to determine if any flaw growth occurs due to a room temperature stress cycle at about the maximum operating stress level of 98 to 105 ksi for an initial flaw size that would just pass a cryogenic proof test. Figure 4 presents the data obtained during this testing phase. Four specimens were stressed to 80, 100, 120 and 140 ksi, respectively, at room temperature. These stress levels were chosen to bracket the maximum operating stresses of 98 to 105 ksi. Three specimens (#7, #9 and #15) exhibited no flaw growth on being loaded to 100, 80 and 140 ksi, respectively. Specimen #12, loaded to 120 ksi, appeared to have a trace of growth. A no growth at room temperature line can be estimated at specimen #12 as indicated in Figure 4. Based on this limited data it appears that no measurable growth could take place at 105 ksi for flaw sizes equal to that which would just pass a cryogenic proof test.

Part IV

The objective of this phase of the program was to determine if any flaw growth occurs due to a room temperature stress cycle to about 98 to 105 ksi after having successfully passed a -320°F proof test to 168 ksi. Figure 5 presents the data obtained during this testing phase. A total of four specimens were tested. As previously discussed in Part II, specimens #14 and #8 exhibited significant flaw growth as shown in Figure 6. The growth present in specimen #14 is believed to have occurred during proof testing and the subsequent room temperature stress cycle, while the growth in specimen #8 is believed to have occurred only during proof testing. The probable growth path for both these specimens is indicated in Figure 5. These growth paths are based on knowing the initial flaw sizes, final flaw sizes after growth, stresses and the amount of crack opening displacement that took place. The results of Part II also played an important role in establishing these paths. The back side (opposite the flaw front) of specimen #14 was

observed during the application of the room temperature stress cycle. Upon reaching 120 ksi stress, the dimple on the back side (already present from passing the cryogenic proof) was observed to become very sharp, indicating the flaw had almost broken through the back surface. This conclusion was born out after marking and failing the specimen and observing the amount of growth that did take place.

The results of specimens #14 and #8 are somewhat academic since neither specimen would have successfully passed a 168 ksi cryogenic proof test. The cryogenic proofs were terminated for both specimens prior to 168 ksi, and in addition, the room temperature stress cycle applied to specimen #14 was 120 ksi which is above the maximum operating stress of 98 to 105 ksi. These specimen do bracket the growth that can take place during cryogenic proof and a subsequent room temperature stress cycle.

From the data obtained during this program, it appears that a specimen or pressure vessel can successfully pass a cryogenic proof test to 168 ksi (having some flaw growth but less than critical) and then successfully be stressed to 105 ksi at room temperature without any additional measurable flaw growth. The cryogenic proof serves its purpose in screening the maximum flaw that can be in the pressure vessel. If, however, a room temperature proof cycle (approximately 140 ksi) is put on the vessel after a cryogenic proof to 168 ksi has been performed, flaw growth can be expected during this room temperature proof. It is considered possible that this additional growth could be sufficient to reduce the vessel capability to a point significantly less than that proven by the prior cryogenic test.

5.0 CONCLUSIONS

1) The plane strain fracture toughness (based on initial flaw sizes) for the Apollo tank material investigated has an average value of 43.2 ksi $\sqrt{in}$ at -320°F in liquid nitrogen.

2) Flaw growth does occur during cryogenic testing at -320°F when the stress intensity exceeds about 85 percent of the K_{Ic} at -320°F.

3) Because of insufficient data, the maximum flaw size after cryogenic proof to 168 ksi at -320°F could not be quantitatively determined.

4) Reduced pressure vessel capability can be expected if the vessel just passes a 168 ksi cryogenic proof test at -320°F and is then subjected to a room temperature proof test to 140 ksi (i.e., the room temperature proof test must then be used in subsequent life estimates).

5) No measurable flaw growth results when a pressure vessel is subjected to a room temperature stress of 105 ksi after barely passing a 168 ksi cryogenic proof test at -320°F. The maximum flaw that exists in the pressure vessel is the one screened by the cryogenic proof test.

REFERENCES

1. Masters, J. N., Haese, W. P. and Finger, R. W., "Investigation of Deep Flaws in Thin Walled Tanks", NASA CR-72606 dated January, 1970.

2. Tiffany, C. F., Masters, J. N. and Bixler, W. D., "Flaw Growth of 6Al-4V Titanium in a Freon TF Environment, " NASA CR-99632, dated April, 1969.

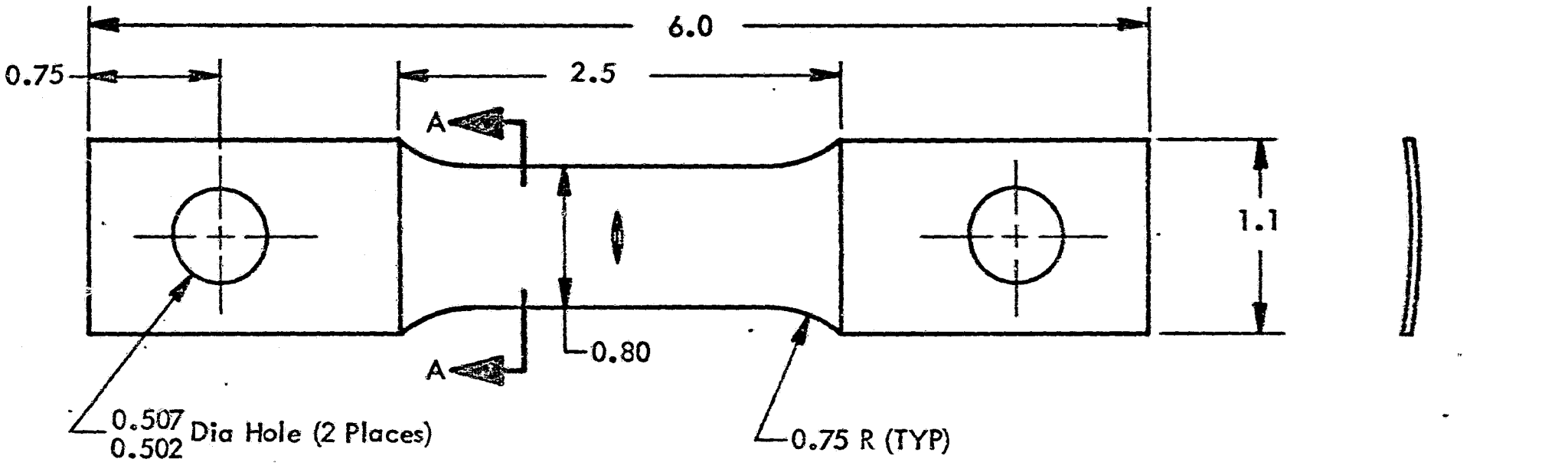

Figure 1: SPECIMEN CONFIGURATION

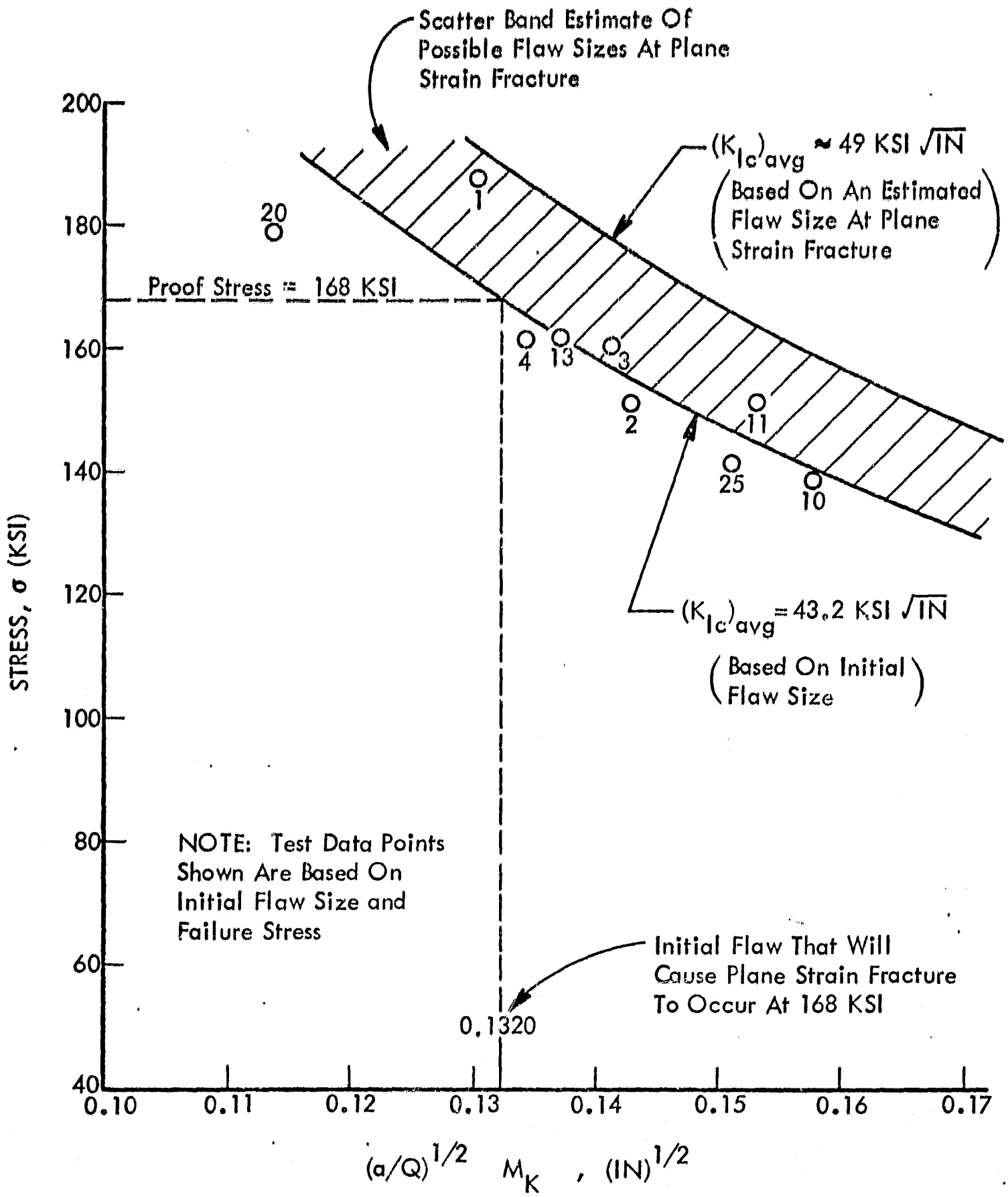

Figure 2: FRACTURE TOUGHNESS AT -320°F

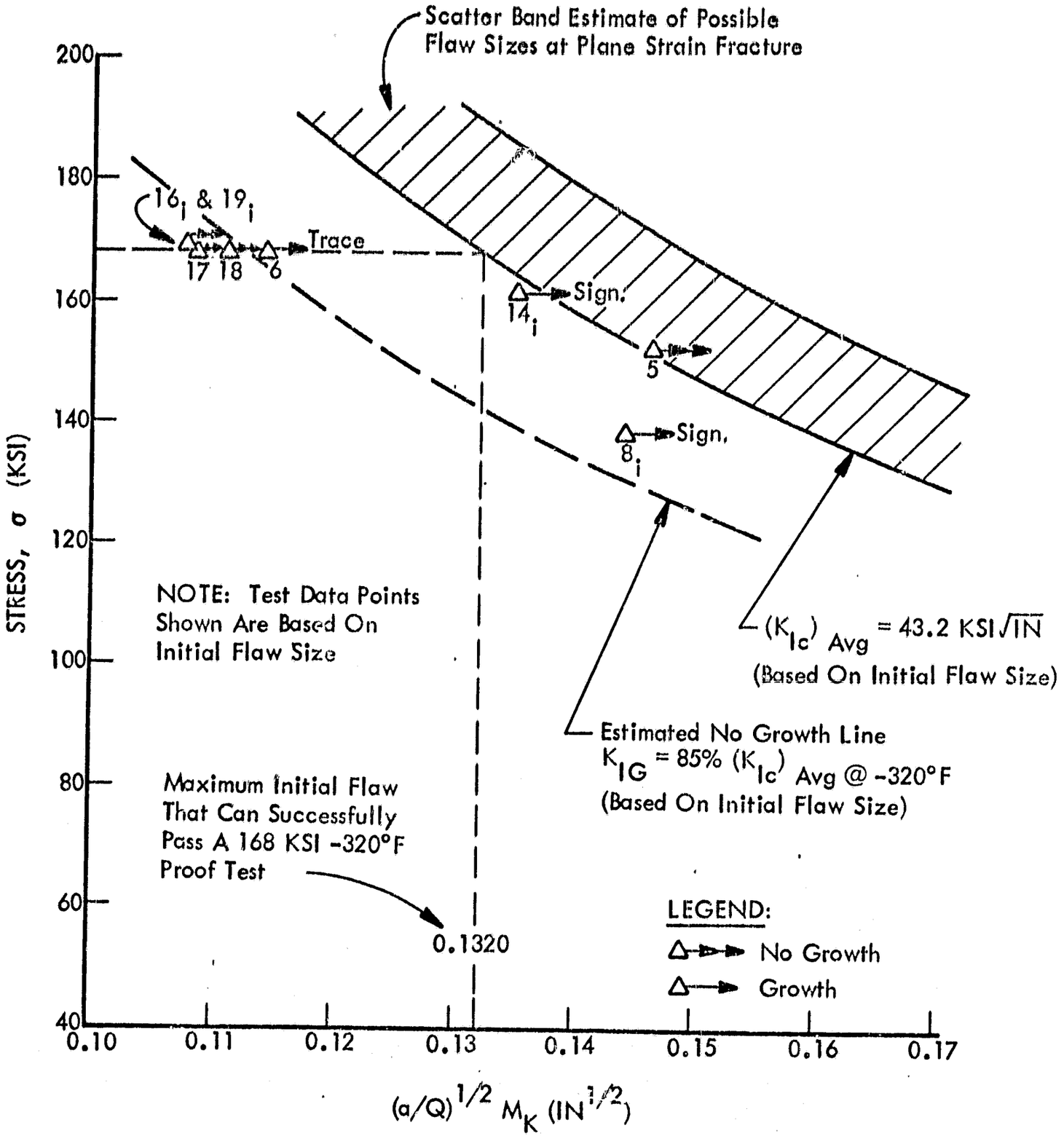

Figure 3: SPECIMENS LOADED TO A -320°F PROOF

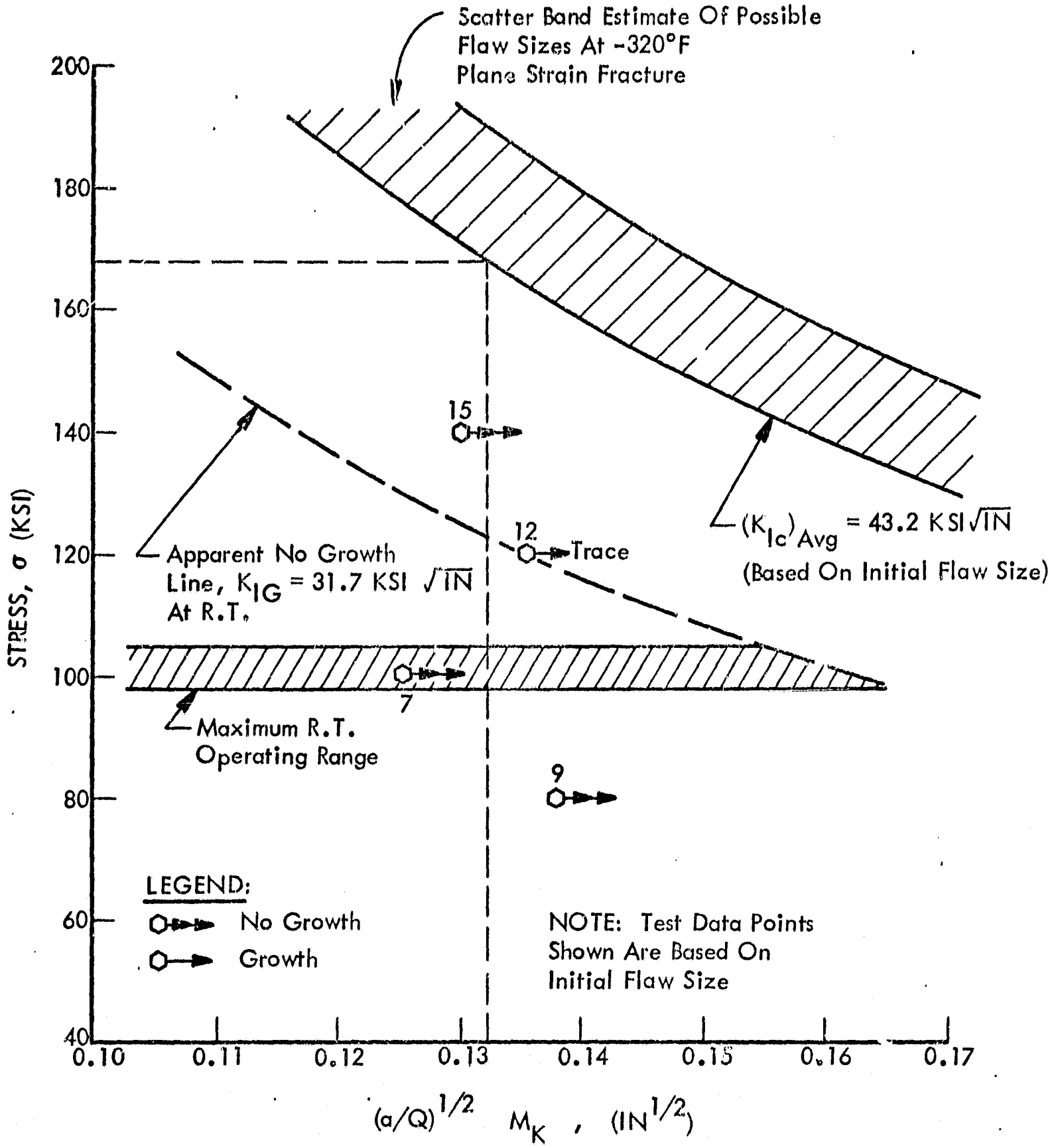

Figure 4: SPECIMENS LOADED AT ROOM TEMPERATURE

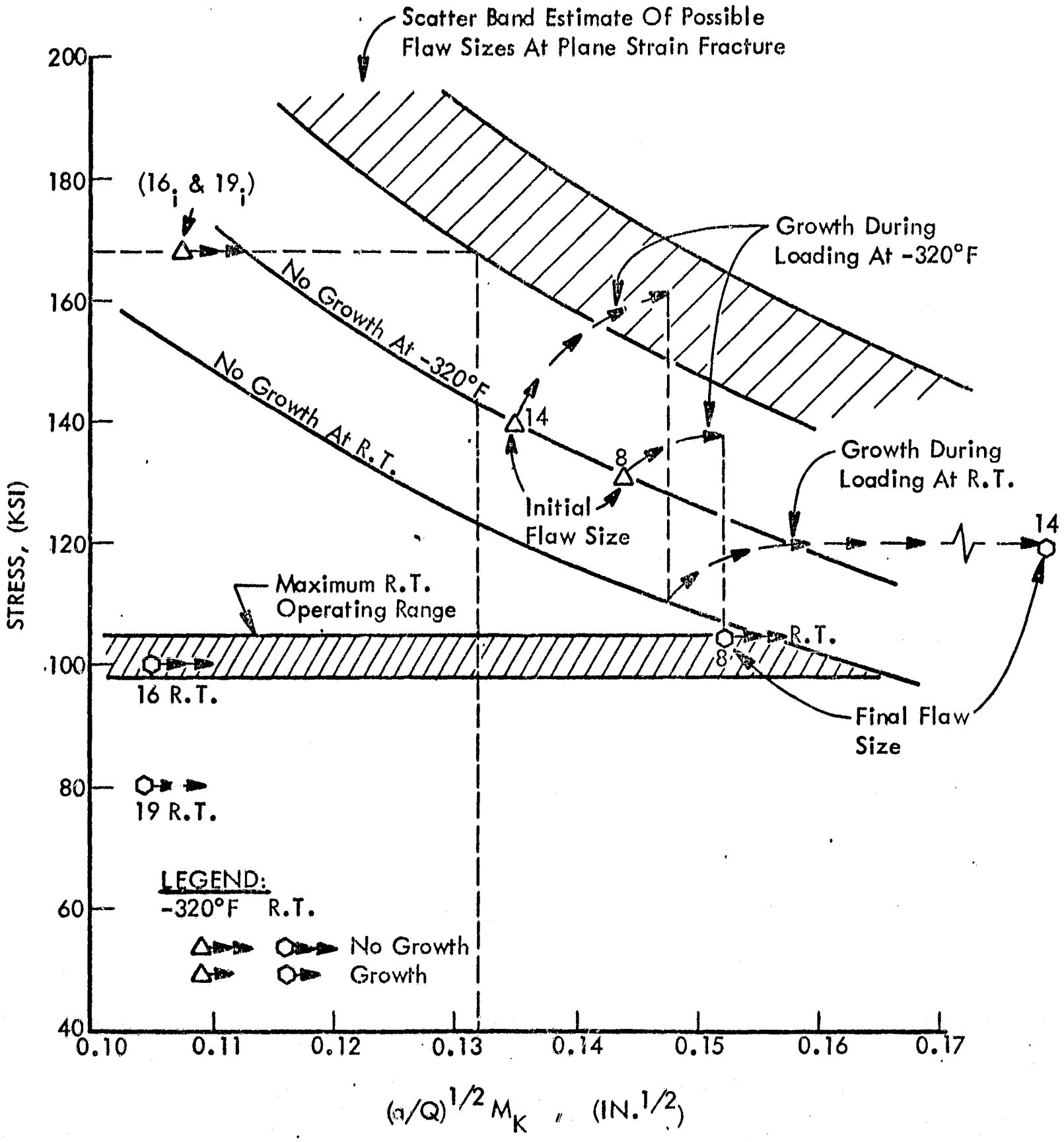

Figure 5: SPECIMENS LOADED TO A -320°F PROOF AND THEN SUBJECTED TO A ROOM TEMPERATURE STRESS CYCLE

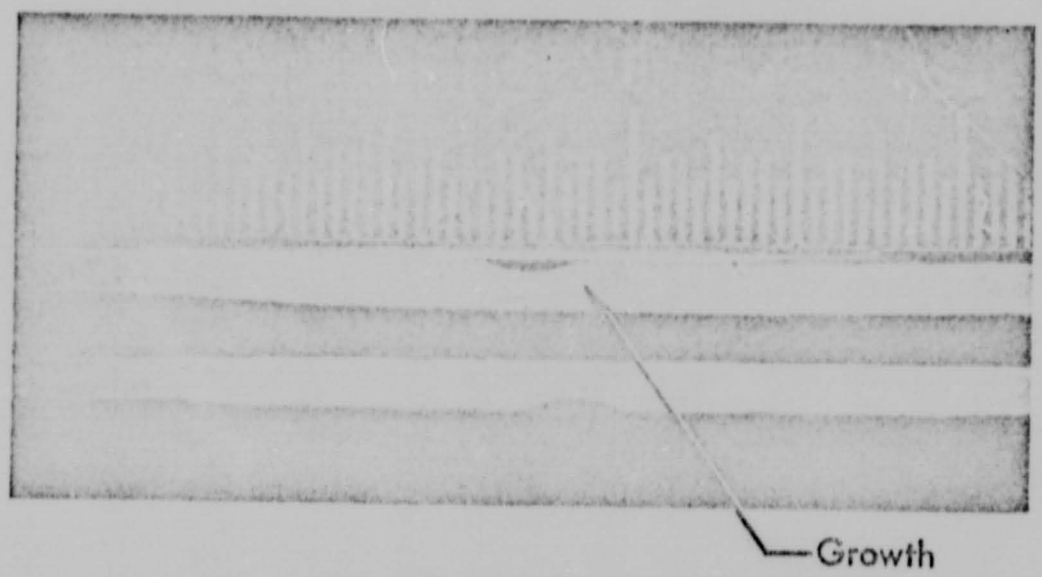

SPECIMEN 14

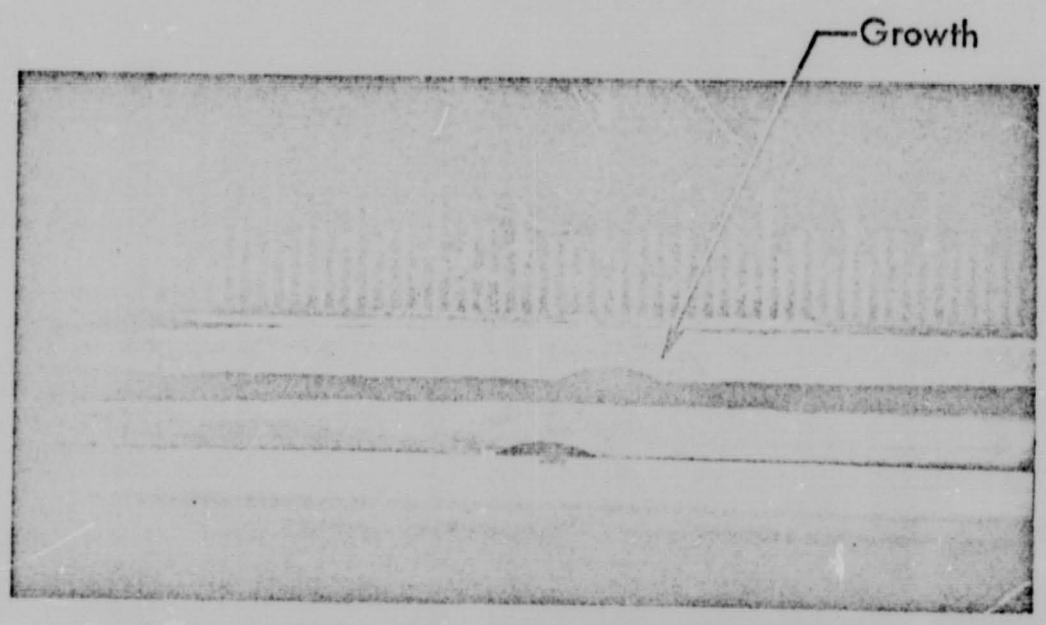

SPECIMEN 8

Figure 6: FRACTOGRAPHS OF SPECIMENS SHOWING SIGNIFICANT GROWTH

Table I: PLANE STRAIN FRACTURE TOUGHNESS OF 6Al-4V S.T.A. TITANIUM AT -320°F

SPECIMEN NUMBER	THICKNESS, t (Inch)	FLAW DEPTH, a (Inch)	FLAW WIDTH, 2c (Inch)	a/2c	STRESS, σ_G (Ksi)	YIELD STRENGTH, σ_{ys} (Ksi)	σ_G/σ_{ys}	FLAW SHAPE PARAMETER, Q	FLAW SIZE, a/Q (Inch)	$(a/Q)^{1.2}$	a/t	M_K	TEST TEMP. (°F)	TEST ENVIRONMENT	K_{Ic} [1] (Ksi $\sqrt{in}$)	$(a/Q)^{1.2} M_K$
25	0.0325	0.0190	0.093	0.204	141.4	220	0.643	1.246	0.0153	0.1236	0.585	1.222	-320	LN_2	41.7	0.1510
1	0.0316	0.0160	0.069	0.232	187.7	220	0.853	1.257	0.0127	0.1129	0.506	1.153	-320	LN_2	47.7	0.1303
2	0.0332	0.0190	0.076	0.250	151.2	220	0.687	1.364	0.0139	0.1180	0.572	1.209	-320	LN_2	42.1	0.1428
3	0.0332	0.0180	0.082	0.2195	160.4	220	0.739	1.258	0.0143	0.1197	0.541	1.181	-320	LN_2	44.2	0.1412
4	0.0321	0.0170	0.073	0.2330	161.5	220	0.734	1.298	0.0131	0.1146	0.530	1.172	-320	LN_2	42.3	0.1341
10	0.0328	0.0225	0.072	0.3125	138.8	220	0.631	1.588	0.0142	0.1190	0.686	1.325	-320	LN_2	42.6	0.1577
11	0.0322	0.0210	0.073	0.2880	151.5	220	0.689	1.488	0.0141	0.1189	0.652	1.289	-320	LN_2	45.2	0.1531
13	0.0334	0.0190	0.066	0.2880	162.0	220	0.736	1.473	0.0130	0.1136	0.569	1.205	-320	LN_2	43.2	0.1370
20	0.0305	0.0130	0.060	0.2170	179.0	220	0.814	1.226	0.0106	0.1030	0.427	1.102	-320	LN_2	39.6	0.1135

Average K_{Ic} = 43.2 KSI $\sqrt{in}$

[1] BASED ON INITIAL FLAW SIZE AND FAILURE STRESS

Table II: SPECIMENS LOADED TO A -320°F PROOF

SPECIMEN NUMBER	THICKNESS, t (Inch)	FLAW DEPTH, a (Inch)	FLAW WIDTH, 2c (Inch)	a/2c	STRESS, σ_G (Ksi)	YIELD STRENGTH, σ_{ys} (Ksi)	σ_G/σ_{ys}	SHAPE PARAMETER, Q	FLAW SIZE, a/Q (Inch)	$(a/Q)^{1/2}$	a/t	M_K	TEST TEMP. (°F)	TEST ENVIRONMENT	K_{Ii} [1] (Ksi $\sqrt{in}$)	AMOUNT OF GROWTH	$(a/Q)^{1/2} M_K$
5	0.0332	0.0190	0.084	0.2261	152.2	220	0.692	1.294	0.0147	0.1211	0.572	1.208	-320	LN_2	43.4	NONE	0.1462
6	0.0323	0.0140	0.058	0.2415	168.0	220	0.763	1.316	0.0106	0.1031	0.434	1.106	-320	LN_2	37.4	TRACE	0.1140
17	0.0316	0.0120	0.062	0.1936	168.0	220	0.763	1.184	0.0101	0.1006	0.380	1.078	-320	LN_2	35.5	NONE	0.1083
18	0.0332	0.0130	0.060	0.2166	168.0	220	0.763	1.244	0.0104	0.1022	0.392	1.083	-320	LN_2	36.4	NONE	0.1108

[1] BASED ON INITIAL FLAW SIZE

Table III: SPECIMENS LOADED AT ROOM TEMPERATURE

SPECIMEN NUMBER	THICKNESS, t (Inch)	FLAW DEPTH, a (Inch)	FLAW WIDTH, 2c (Inch)	a/2c	STRESS, σ_G (Ksi)	YIELD STRENGTH, σ_{ys} (Ksi)	σ_G/σ_{ys}	SHAPE PARAMETER, Q	FLAW SIZE, a/Q (Inch)	$(a/Q)^{1/2}$	a/t	M_K	TEST TEMP. (°F)	TEST ENVIRONMENT	K_{Ii} (Ksi $\sqrt{in}$) [1]	AMOUNT OF GROWTH	$(a/Q)^{1/2} M_K$
7	0.0330	0.0160	0.069	0.232	100.0	155	0.645	1.323	0.0121	0.1100	0.485	1.140	RT	AIR	24.5	NONE	0.1254
9	0.0335	0.0190	0.073	0.2610	80.1	155	0.517	1.442	0.0132	0.1148	0.567	1.202	RT	AIR	21.6	NONE	0.1380
12	0.0328	0.0180	0.068	0.265	120.0	155	0.775	1.384	0.0130	0.1141	0.549	1.188	RT	AIR	31.8	TRACE	0.1356
15	0.0312	0.0160	0.065	0.2462	140.0	155	0.904	1.276	0.0125	0.1120	0.513	1.160	RT	AIR	35.5	NONE	0.1300

[1] BASED ON INITIAL FLAW SIZE

Table IV: SPECIMENS LOADED TO A -320°F PROOF AND THEN SUBJECTED TO A ROOM TEMPERATURE STRESS CYCLE

SPECIMEN NUMBER	THICKNESS, t (Inch)	FLOW DEPTH, a (Inch)	FLOW WIDTH, 2c (Inch)	a/2c	STRESS, σ_G (Ksi)	YIELD STRENGTH, σ_{ys} (Ksi)	σ_G/σ_{ys}	SHAPE PARAMETER, Q	FLAW SIZE, a/Q (Inch)	$(a/Q)^{1/2}$	a/t	M_K	TEST TEMP. (°F)	TEST ENVIRONMENT	K_{Ii} (Ksi $\sqrt{in}$)	AMOUNT OF GROWTH	$(a/Q)^{1/2} M_K$
8i	0.0330	0.0195	0.074	0.264	138.7	220	0.628	1.424	0.137	0.1171	0.591	1.228	-320	LN_2	38.8	SIGN.	0.1439
8f	0.0330	0.0210	0.075	0.280	105.0	155	0.678	1.464	0.0144	0.1198	0.637	1.270	RT	AIR	31.2	NONE	0.1521
14i	0.0315	0.0185	0.061	0.3035	161.5	220	0.735	1.528	0.0121	0.1100	0.582	1.223	-320	LN_2	42.5	SIGN.	0.1347
14f	0.0315	0.0260	0.080	0.3255	120.0	155	0.774	1.592	0.0163	0.1278	0.825	1.486	RT	AIR	44.4	SIGN.	0.1900
16i	0.0331	0.0120	0.060	0.200	163.0	220	0.764	1.182	0.0102	0.1008	0.363	1.070	-320	LN_2	35.4	NONE	0.1079
16f	0.0331	0.0120	0.060	0.200	100.0	155	0.645	1.235	0.0097	0.0986	0.363	1.070	RT	AIR	20.6	NONE	0.1055
19i	0.0319	0.0120	0.060	0.200	167.8	220	0.764	1.201	0.0100	0.1000	0.376	1.075	-320	LN_2	35.2	NONE	0.1075
19f	0.0319	0.0120	0.060	0.200	80.0	155	0.516	1.266	0.0095	0.0974	0.376	1.075	RT	AIR	16.4	NONE	0.1047

NOTE: i INDICATES CALUCLATIONS ARE BASED ON INITIAL FLAW SIZE AT PROOF WHILE

f INDICATES CALCULATIONS ARE BASED ON FINAL FLAW SIZE AT R.T. OPERATING STRESS